

See discussions, stats, and author profiles for this publication at: <https://www.researchgate.net/publication/384455117>

PID-Fixed Time Sliding Mode Control for Trajectory Tracking of AUVs Under Disturbance

Conference Paper · April 2024

CITATIONS

0

READS

56

3 authors, including:



Jack Close

Queen's University Belfast

5 PUBLICATIONS 4 CITATIONS

SEE PROFILE

PID-Fixed Time Sliding Mode Control for Trajectory Tracking of AUVs under Disturbance

Jack Close * Mien Van * Stephen McIlvanna *

* School of Electronics, Electrical Engineering and Computer Science,
Queen's University Belfast, BT7 1NN, Northern Ireland

Abstract: A novel approach is proposed for the trajectory tracking control of Autonomous Underwater Vehicles (AUVs). Firstly, previous implementations of Proportional-Integral-Derivative (PID) and Sliding Mode Control (SMC) are discussed and their disadvantages are highlighted in terms of fixed time convergence and the chattering phenomenon. Secondly, to improve the stability of the tracking performance and convergence of the system, a controller combining PID and Fixed Time SMC (FTSMC) is proposed for AUVs. The proposed controller is then applied to simulate a 6 Degrees-of-Freedom (6DOF) BlueRov2 underwater robot and the results are analytically discussed. The simulation results show that the proposed PID-FTSMC controller can accurately control the BlueRov2 in trajectory tracking operations with faster convergence and no oscillations around the set reference, even under disturbance.

Keywords: Autonomous Underwater Vehicles, Sliding Mode Control, Robust Control, Guidance Navigation and Control

1. INTRODUCTION

The world of Robotics has grown over the past decades to a level where Unmanned Vehicles are not just feasible but now have massive impacts when implemented across many sectors. This is especially true in Marine Robotics, where research focuses on developing control methods for the emerging technology, Autonomous Underwater Vehicles (AUVs) - “self-propelled, unmanned, untethered underwater vehicles capable of carrying out simple activities with little or no human supervision” - Bellingham (2009). AUVs are crucial for tasks such as defence operations - Knight (2024), marine geoscience - Zhu et al. (2018), the oil and gas industries - Bharti et al. (2018), and environmental monitoring - Horimoto et al. (2018). However, AUV technology still has current shortcomings that need addressed, driving the development of more sophisticated control strategies. Proportional-Integral-Derivative (PID) controllers, due to their simplicity and effectiveness, have been developed for AUVs (Sarhadi et al. (2016), Lipko (2023)). The main goal of implementing PID into a system is to maintain a desired set point by adjusting the system’s input responses. Using state feedback, the error is directly tracked for the P component, integrated for the I component, and differentiated for the D component for convergence and oscillation (due to potential overshooting) control. PID controllers have constants known simply as ‘Controller Gains’ that need manual tuning, often through trial and error. Fractional-order PID controllers, proposed in Liu et al. (2022) and Ajmal et al. (2014), are more complex with the addition of fractional calculus, offering more tuning freedom.

Robotic control in underwater environments must consider model uncertainties and disturbances that can nega-

tively affect performance. Robust control schemes, such as Sliding Mode Control (SMC), have been extensively researched for AUVs due to their strength against uncertainty (Qin et al. (2023), Mudassir and Memon (2020), Gomez et al. (2020)). Integral Sliding Mode Control (ISMC) has been explored for Marine Surface Vehicles (MSVs) to eliminate the reaching phase of SMC, Van (2019b), applicable to systems with more Degrees of Freedom (DOF) like a 6DOF AUV. SMC’s tracking performance can be enhanced by integrating Neural Networks or Fuzzy Logic Control, which are based on learning algorithms (Tang et al. (2022), Zhu et al. (2023), Van (2019a)). The chattering phenomenon, a drawback of conventional SMC, causes high-frequency oscillations in control signals, Boiko (2023), leading to wear and inefficient energy consumption. Fixed-time Sliding Mode Control (FTSMC) has been studied to address these issues, incorporating a nonlinear sliding variable for finite time convergence and smoother control input transitions, promoting longevity and efficiency in AUV operations. FTSMC can eliminate chattering depending on its application but if this can’t be achieved, the chattering still experiences a reduction.

Higher-order SMC (HOSMC) has shown great performance in reducing chattering - Van et al. (2014). However, combining PID with FTSMC to preserve high tracking performance, fast convergence, and eliminate chattering has not been explored.

To fill this gap, a novel PID-FTSMC AUV Controller is proposed. Initially, an SMC framework for AUVs is developed. Then, a unified PID-FTSMC controller is designed to overcome convergence and chattering drawbacks. The stability of the PID-FTSMC is rigorously analysed, and simulations are conducted on a 6DOF BlueRov2 model, with results analysed. This paper is structured as follows:

Section 2 presents the Dynamic Modelling of a BlueRov2 AUV. Section 3 explains the proposed PID-FTSMC theory and Stability Analysis. Section 4 provides Simulation Results. Section 5 concludes the paper's findings.

2. DYNAMIC MODELLING OF BLUEROV2

Based on the standard set by the Society of Naval Architects and Marine Engineers, SNAME (1950), the nomenclature attributed to each 6DOF variable for an AUV is defined in Table 1.

Table 1. Standard Notation for Marine Vessels (SNAME) (1950)

Degree of Freedom	Pose / Angle	Velocity / Angular Velocity	Force / Moment
Surge	x_b	v_{xb} , u	X
Sway	y_b	v_{yb} , v	Y
Heave	z_b	v_{zb} , w	Z
Roll	ϕ	v_ϕ , p	K
Pitch	θ	v_θ , q	M
Yaw	ψ	v_ψ , r	N

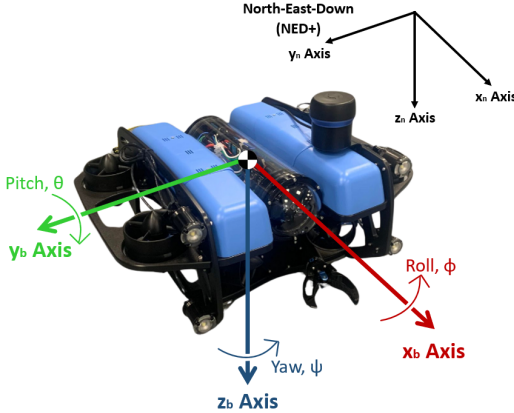


Fig. 1. 6 Degrees of Freedom for the BlueRov2 platform

For the AUV platform, the North-East-Down (NED) convention is used with the AUV's volumetric centre at (x_n, y_n, z_n) as shown in Figure 1. The Pose Vector $\eta = (x_b, y_b, z_b, \phi, \theta, \psi)^T \in \mathbb{R}^6$ includes the 3D coordinates of the robot's centre $(x_b, y_b, z_b)^T$ (m) and the orientation angles $(\phi, \theta, \psi)^T$ (rad) around the x, y, z axes. The Velocity Vector $\mu = (u, v, w, p, q, r)^T \in \mathbb{R}^6$ contains the directional velocities $(u, v, w)^T$ (m/s) and angular velocities $(p, q, r)^T$ (rad/s) representing turn rates around the x, y, z axes. The BlueRov2 platform's total state is $\xi = [\eta^T, \mu^T]$. Forces and moments acting on the BlueRov2 are given by $(X, Y, Z, K, M, N)^T$. Linear forces $(X, Y, Z)^T$ (N) and moments $(K, M, N)^T$ (Nm) represent torques around the x, y, z axes. The AUV's control inputs are $\tau = (\tau_x, \tau_y, \tau_z, \tau_\phi, \tau_\theta, \tau_\psi)^T \in \mathbb{R}^6$, where (τ_x, τ_y, τ_z) (N) are Control Forces and $(\tau_\phi, \tau_\theta, \tau_\psi)$ (Nm) are Control Torques.

2.1 Kinematic Model

The following Kinematic and Kinetic Matrices have incorporated constants which can be found in Table 2.

Equation (1) is the Kinematic Formula of a 6DOF AUV used for calculating the pose states in the next time

Table 2. Constants used in BlueRov2 Dynamic Modelling

Constant	Value	Units
m	11.5	kg
W	112.8	N
B	114.8	N
I_x	0.16	kgm^2
I_y	0.16	kgm^2
I_z	0.16	kgm^2
$X_{\dot{u}}$	-5.5	kg
$Y_{\dot{v}}$	-12.7	kg
$Z_{\dot{w}}$	-14.57	kg
K_p	-0.12	kgm^2/rad
M_q	-0.12	kgm^2/rad
N_r	-0.12	kgm^2/rad
X_u	-4.03	Ns/m
Y_v	-6.22	Ns/m
Z_w	-5.18	Ns/m
K_p	-0.07	Ns/rad
M_q	-0.07	Ns/rad
N_r	-0.07	Ns/rad
$X_u + X_{ u u} u $	-18.18	Ns^2/m^2
$Y_v + Y_{ v v} v $	-21.66	Ns^2/m^2
$Z_w + Z_{ w w} w $	-36.99	Ns^2/m^2
$K_p + K_{ p p} p $	-1.55	Ns^2/rad^2
$M_q + M_{ q q} q $	-1.55	Ns^2/rad^2
$N_r + N_{ r r} r $	-1.55	Ns^2/rad^2

step and can be found in the Handbook of Marine Craft Hydrodynamics and Motion Control (pg. 30) in Fossen (2011), this provided the foundational theory in which the Kinematic and Kinetic Matrices that comprise the full dynamic model were constructed.

$$\dot{\eta} = J(\eta)\mu \quad (1)$$

The **Jacobian Transformation Matrix** (2) exists to combine the Linear (3) and Angular (4) Rotation Matrices which in turn transform the linear and angular velocities of the AUV from its own Body-fixed frame to the environment's Earth-fixed frame.

$$J(\eta) = \begin{bmatrix} R_b^n(\Theta) & 0_{3 \times 3} \\ 0_{3 \times 3} & T(\Theta) \end{bmatrix} \quad (2)$$

The **Linear Rotation Matrix** (3) converts the linear velocities experienced by the AUV from its own Body-fixed frame to the environment's Earth-fixed frame.

$$R_b^n(\Theta) = \begin{bmatrix} C\psi C\theta & -S\psi C\phi + C\psi S\theta S\phi & S\psi S\phi + C\psi C\phi S\theta \\ S\psi C\theta & C\psi C\phi + S\phi S\theta S\psi & -C\psi S\phi S\theta S\psi C\phi \\ -S\theta & C\theta S\phi & C\theta C\phi \end{bmatrix} \quad (3)$$

Where $C = \cos$; $S = \sin$.

The **Angular Rotation Matrix** (4) transforms the angular velocities of the AUV from its own Body-fixed frame to the environment's Earth-fixed frame.

$$T(\Theta) = \begin{bmatrix} 1 & \sin \phi \tan \theta & \cos \phi \tan \theta \\ 0 & \cos \phi & -\sin \phi \\ 0 & \sin \phi & \cos \phi \\ 0 & \frac{\cos \theta}{\cos \phi} & \frac{\cos \theta}{\cos \phi} \end{bmatrix} \quad (4)$$

2.2 Kinetic Model

From the Handbook of Marine Craft Hydrodynamics and Motion Control (pg. 171) Fossen (2011), equation (5)

below is the nonlinear equation of motion for a 6DOF AUV.

$$\tau = M_{Total}\dot{\mu} + C_{Total}\mu + D(\mu)\mu + g(\eta) \quad (5)$$

Equation (6) combines the Added (7) and the Rigid Body (8) Mass Matrices to form the **Total Mass Matrix**.

$$M_{Total} = M_A + M_{RB} \quad (6)$$

The **Added Mass Matrix** (7) calculates the **added mass force** along the respective axis caused by the acceleration in any of the AUV's 6DOF.

$$M_A = -\text{diag}[X_{\dot{u}} \ Y_{\dot{v}} \ Z_{\dot{w}} \ K_{\dot{p}} \ M_{\dot{q}} \ N_{\dot{r}}] \quad (7)$$

The **Rigid Body Mass Matrix** (8) calculates the **inertia that the AUV experiences due to its own mass**. It includes the mass of the AUV, m , the moments experienced due to momentum and inertia around the x,y,z axes (I_x, I_y, I_z) and also accounts for the distance between the AUV's Centre of Mass and the origin of the Body-fixed frame.

$$M_{RB} = \begin{bmatrix} m & 0 & 0 & 0 & mz_g & 0 \\ 0 & m & 0 & -mz_g & 0 & 0 \\ 0 & 0 & m & 0 & 0 & 0 \\ 0 & -mz_g & 0 & I_x & 0 & 0 \\ mz_g & 0 & 0 & 0 & I_y & 0 \\ 0 & 0 & 0 & 0 & 0 & I_z \end{bmatrix} \quad (8)$$

Equation (9) forms the **Total Coriolis Effect Matrix**:

$$C_{Total} = C_A(\mu) + C_{RB}(\mu) \quad (9)$$

The **Added Centripetal and Coriolis Force Skew Matrix** (10) calculates the **rotational inertia experienced by the AUV** which is caused by the Earth's natural rotation, impacting the Earth-fixed frame.

$$C_A(\mu) = \begin{bmatrix} 0 & 0 & 0 & 0 & Z_{\dot{w}}w & 0 \\ 0 & 0 & 0 & -Z_{\dot{w}}w & 0 & 0 \\ 0 & 0 & 0 & -Y_{\dot{v}}v & X_{\dot{u}}u & 0 \\ 0 & -Z_{\dot{w}}w & Y_{\dot{v}}v & 0 & -N_{\dot{r}}r \ M_{\dot{q}}q & \\ Z_{\dot{w}}w & 0 & -X_{\dot{u}}u & N_{\dot{r}}r & 0 & -K_{\dot{p}}p \\ -Y_{\dot{v}}v & X_{\dot{u}}u & 0 & -M_{\dot{q}}q & K_{\dot{p}}p & 0 \end{bmatrix} \quad (10)$$

The **Rigid Body Centripetal and Coriolis Force Matrix** (11) calculates the **rotational inertia experienced by the AUV** which is caused by its own linear and rotational accelerations.

$$C_{RB}(\mu) = \begin{bmatrix} 0 & 0 & 0 & 0 & mw & 0 \\ 0 & 0 & 0 & -mw & 0 & 0 \\ 0 & 0 & 0 & mv & -mu & 0 \\ 0 & -mw & mv & 0 & I_{zr} - I_{yq} & \\ mw & 0 & -mu - I_{zr} & 0 & I_{xp} & \\ mv - mu & 0 & I_{yq} & -I_{xp} & 0 & \end{bmatrix} \quad (11)$$

The **Hydrodynamic Damping Matrix** (12) calculates the **linear and quadratic hydro-damping** experienced by the AUV. These damping effects arise due to Skin Friction and Vortex Shredding when the AUV is in motion underwater.

$$D(\mu) = -\text{diag}[D_{11} \ D_{22} \ D_{33} \ D_{44} \ D_{55} \ D_{66}] \quad (12)$$

Where,

$$\begin{aligned} D_{11} &= X_u + X_{|u|u}|u|, \\ D_{22} &= Y_v + Y_{|v|v}|v|, \\ D_{33} &= Z_w + Z_{|w|w}|w|, \\ D_{44} &= K_p + K_{|p|p}|p|, \\ D_{55} &= M_q + M_{|q|q}|q|, \\ D_{66} &= N_r + N_{|r|r}|r|. \end{aligned}$$

The **Hydrostatic Force Matrix** (13) represents the **restoring forces and moments** about the AUV's Centre of Mass which are caused by the combination of the upwards force (buoyancy) of the AUV and the downwards force (gravity) imposed on it.

$$g(\eta) = \begin{bmatrix} (W - B) \sin \theta \\ -(W - B) \cos \theta \sin \phi \\ -(W - B) \cos \theta \cos \phi \\ z_g W \cos \theta \sin \phi \\ z_g W \sin \theta \\ 0 \end{bmatrix} \quad (13)$$

Where $B = \rho g \nabla$; $W = mg$

3. PID-FTSMC CONTROLLER DESIGN

This section describes the controller based on PID-FTSMC. It is necessary to remember the Kinematic Formula and Nonlinear Equation of motion which are critical equations in Section 2.

$$\dot{\eta} = J(\eta)v \quad (1)$$

$$\tau = M_{Total}\dot{\mu} + C_{Total}\mu + D(\mu)\mu + g(\eta) \quad (5)$$

3.1 Design of PID-FTSMC controller

Below are details on the design of the controller based on PID-FTSMC such that the system's states, i.e., η , can track the desired trajectory, i.e., $\eta = \eta_{ref} = [x_{ref} \ y_{ref} \ z_{ref} \ \phi_{ref} \ \theta_{ref} \ \psi_{ref}]^T$, accurately. To fulfil this objective, the tracking positional and velocity errors for 6DOF denoted by e and \dot{e} are defined as $e = \eta - \eta_{ref}$ and $\dot{e} = \mu - \mu_{ref}$, respectively. To combine the position/velocity tracking errors, e and \dot{e} , the following Sliding Surface, s , is formulated:

$$s = \dot{e} + k_1 |e|^\alpha + k_2 |e|^\gamma \quad (14)$$

Where,

$$\begin{aligned} |e|^\alpha &= |e|^\alpha \text{sign}(e), \\ |e|^\gamma &= |e|^\gamma \text{sign}(e). \end{aligned}$$

It is then possible to incorporate PID control on this Sliding Surface to restore unexpected deviation and drive the system's states to stability. The equation becomes:

$$s_{PID} = k_p s(t) + k_i \int_0^t s(t)dt + k_d \frac{ds(t)}{dt} \quad (15)$$

Remark 1: The selection of the new Sliding Surface in (15) based on the PID method provides two advantages: (i) it preserves the properties of the PID controller, and (ii) it increases the order of the dynamic system. Therefore, it can preserve the HOSMC property, which increases the tracking performance, while reducing chattering. This is the main novelty of this paper.

Determining $\frac{ds(t)}{dt}$ is necessary for the Derivative portion of PID control and this can be calculated by differentiating Equation (14).

$$\frac{ds(t)}{dt} = \ddot{e} + k_1\alpha|e|^{\alpha-1}\dot{e} + k_2\gamma|e|^{\gamma-1}\dot{e} \quad (16)$$

Where,

$$\begin{aligned} e &= \eta - \eta_{ref}, \\ \dot{e} &= \dot{\eta} - \dot{\eta}_{ref}, \\ \ddot{e} &= \ddot{\eta} - \ddot{\eta}_{ref}. \end{aligned}$$

$\ddot{\eta}$ is the instantaneous acceleration experienced by each 6DOF. It is calculated by applying product rule to Equation (1). From this derivation, a substitution can be made by rearranging Equation (5) for $\dot{\mu}$:

$$\begin{aligned} \ddot{\eta} &= \dot{J}(\eta)\mu + J(\eta)\dot{\mu} \\ &= \dot{J}(\eta)\mu \\ &\quad + J(\eta)(M_{Total}^{-1}(\tau - C(\mu)\mu - D(\mu)\mu - g(\eta))) \end{aligned} \quad (17)$$

By redefining parts of Equation (17) as follows:

$$\Delta = J(\eta)M_{Total}^{-1} \quad (18)$$

$$\Sigma = \dot{J}(\eta)\mu - \Delta(C(\mu) + D(\mu)\mu + g(\eta)) \quad (19)$$

The instantaneous acceleration error, \ddot{e} needed for Equation (16), can be written as:

$$\ddot{e} = \Delta\tau + \Sigma \quad (20)$$

Substituting Equation (20) into Equation (16) provides:

$$\frac{ds(t)}{dt} = \Delta\tau + \Sigma + k_1\alpha|e|^{\alpha-1}\dot{e} + k_2\gamma|e|^{\gamma-1}\dot{e} \quad (21)$$

Which in turn can be substituted back into the s_{PID} formula, Equation (15), to give:

$$\begin{aligned} s_{PID} &= k_p s(t) + k_i \int_0^t s(t) dt + \Delta\tau + \Sigma + \\ &\quad k_1\alpha|e|^{\alpha-1}\dot{e} + k_2\gamma|e|^{\gamma-1}\dot{e} \end{aligned} \quad (22)$$

where $k_d = 1$ is selected for simplicity in analysis.

Let:

$$\begin{aligned} \Gamma &= k_p s(t) + k_i \int_0^t s(t) dt + \Sigma + \\ &\quad k_1\alpha|e|^{\alpha-1}\dot{e} + k_2\gamma|e|^{\gamma-1}\dot{e} \end{aligned} \quad (23)$$

$$\text{Therefore, } s_{PID} = \Gamma + \Delta\tau \quad (24)$$

The control signals generated by the controller, u_{PID} are calculated by:

$$u_{PID} = -\Delta^+(u_{eq} + u_r) \quad (25)$$

Where,

$$u_{eq} = \Gamma$$

To determine u_r , firstly \dot{u}_r can be calculated with Equation (26) and then integrated to obtain u_r :

$$\dot{u}_r = (k_3 + a)\text{sign}(s_{PID}) \quad (26)$$

Where k_3 and a are constants that can be tuned.

3.2 Stability analysis

Theorem 1. If the controller (25) is applied for the system described in (1) and (5), then the stability of the system is guaranteed, and the fixed-time convergence of the system is achieved.

Proof.

Inserting the controller (25) into the Sliding Surface in (24), we have:

$$s_{PID} = -u_r + \Gamma \quad (27)$$

Differentiating (27), we have

$$\dot{s}_{PID} = -\dot{u}_r + \dot{\Gamma} \quad (28)$$

Assumption 1. The model uncertainty and its derivative are bounded by constants, that is:

$$\delta_\Gamma = |\dot{\Gamma}| \leq \zeta \quad (29)$$

Consider a Lyapunov function candidate:

$$V = \frac{1}{2}s_{PID}^T s_{PID} \quad (30)$$

Differentiating (30) and using (28) and (29), we have

$$\begin{aligned} \dot{V} &= s_{PID}^T \dot{s}_{PID} \\ &= s_{PID}^T(-(k_3 + a)\text{sign}(s_{PID}) + \delta_\Gamma) \\ &= -a|s_{PID}| - k_3|s_{PID}| + \delta_\Gamma s_{PID} \end{aligned} \quad (31)$$

From (31), we can see that if we choose a as a small constant and $k_3 > \zeta$, then $\dot{V} < 0$. That guarantees the stability of the system.

On the other hand, when the system converges to zero, then $s_{PID} = 0$. Consequently, from (15), we can obtain $s = 0$. From (14), we have:

$$\dot{e} = -k_1|e|^\alpha - k_2|e|^\gamma \quad (32)$$

Lemma 1: Van et al. (2023) If there exists a positive definite continuous function y such that $\dot{y} = -k_1|y|^\alpha - k_2|y|^\gamma$ for some $k_1 > 0, k_2 > 0, \alpha > 1$, and $0 < \gamma < 1$, then it is globally fixed-time stable and the settling time is bounded by: $T_{max} \leq \frac{1}{k_1(\alpha-1)} + \frac{1}{k_2(1-\gamma)}$.

According to **Lemma 1**, the system guarantees a fixed-time convergence. The convergence time is bounded by:

$$T_{max} \leq \frac{1}{k_1(\alpha-1)} + \frac{1}{k_2(1-\gamma)} \quad (33)$$

Remark 2: In (26), \dot{u}_r contains the *sign* function, which generates chattering. However, when integrating \dot{u}_r to get u_r , u_r becomes a smooth function. Therefore, the chattering phenomenon is eliminated.

Remark 3: As shown in (15), the system performance depends very much on the selection of k_p, k_i and k_d . These parameters need to be tuned online, for example, using a Reinforcement Learning agent.

Remark 4: One of the disadvantages of the proposed approach is that the sliding gain k_3 is selected based on Assumption 1. This issue can be resolved by using a learning method such as a neural network or fuzzy logic

approximations, and this will be considered in our future work.

4. SIMULATION RESULTS

To test the proposed controller, a Simulink model of the PID-FTSMC framework and a BlueRov2 unit were designed. The simulation was at a Fixed Time step of 0.001s and used the ode4 solver.

The framework includes parameters (k_p, k_i, k_1, k_2, k_3 and a) that need tuning for accurate control and trajectory tracking. These parameters, represented as 6x1 vectors, adjust each of the 6DOF independently. For this simulation, their values were determined through trial and error to achieve the desired results. Future work will explore optimal solutions for calculating these parameters.

$$\begin{aligned}k_p &= [275, 275, 275, 25, 25, 25]^T, \\k_i &= [0.5, 0.5, 0.5, 0.1, 0.1, 0.1]^T, \\k_1 &= [50, 50, 50, 10, 10, 10]^T, \\k_2 &= [12, 12, 12, 8, 8, 8]^T, \\k_3 &= [300, 300, 300, 88, 88, 88]^T, \\a &= [1, 1, 1, 1, 1, 1]^T, \alpha = 1, 5, \gamma = 0.8.\end{aligned}$$

A simulated disturbance was added in the BlueRov2 block to test the robustness of the controller. The disturbance profile was:

$$\begin{aligned}x_{Disturb.} &= 1.5u + \sin(3x_b) + 1.5\sin(u) \\y_{Disturb.} &= 1.5v - 2\sin(2y_b) + 1.3\sin(v) \\z_{Disturb.} &= -1.2w - 2\sin(z_b) + 1.13\sin(w) \\phi_{Disturb.} &= 1.5p + \sin(3\phi_b) + 1.5\sin(p) \\theta_{Disturb.} &= 1.5q - 2\sin(2\theta_b) + 1.3\sin(q) \\psi_{Disturb.} &= -1.2r - 2\sin(\psi_b) + 1.13\sin(r)\end{aligned}$$

With the reference trajectory set at:

$$\eta_{ref} = \begin{bmatrix} 6\sin(0.2t_{sim}) + 5 \\ 5\sin(0.2t_{sim} + \frac{\pi}{2}) + 5 \\ 2\sin(0.6t_{sim}) + 5 \\ 0.4 \\ 0.4 \\ 0.4 \end{bmatrix} \quad (34)$$

As seen in Figure 2 the motion completed by the AUV, with an initial position of (0,0,0), shows a smooth trajectory up to the reference path, η_{ref} , and remains on this reference for the remainder of the simulation. The tuned parameters ensure no overshoot, which would be an inaccurate flaw, and instead exhibits smooth motion. Also simulated, to show the importance of the gain values, is the PID-FTSMC where each respective 6DOF receive the same, insubstantial gain value ($k_p = 15_{x6}, k_i = 5_{x6}, k_1 = 10_{x6}, k_2 = 10_{x6}, k_3 = 15_{x6}, a = 20_{x6}$) and the CTC performance.

Figure 3 shows the AUV's pose compared to the reference and the respective tracking error throughout the simulation for all 6DOF. Each spatial and rotational variable starts in its initial state and quickly moves toward its reference point. As the system's state approaches the set point, it converges to the reference smoothly, as observed in Figure 3b, where the error starts at its maximum deviation and rapidly reaches zero, remaining there without chattering. The simulated disturbance does not affect the AUV's

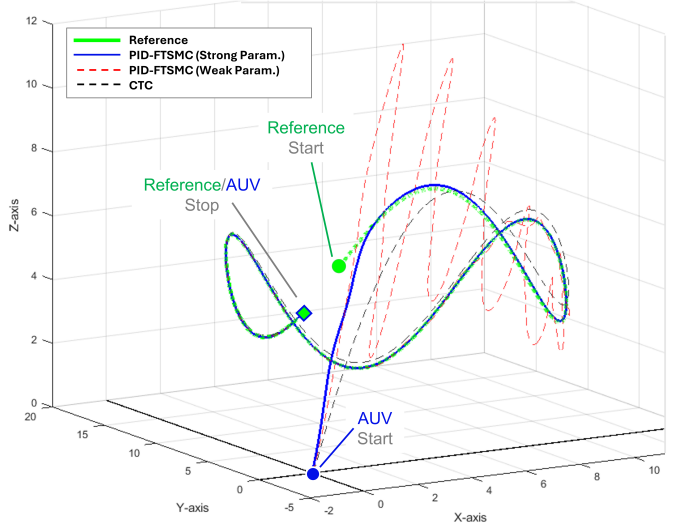


Fig. 2. PID-FTSMC Simulation Results

performance. A comparison with a Computed Torque Controller (CTC) shows the well-tuned PID-FTSMC method converges faster with less overshoot. The badly-tuned PID-FTSMC oscillates for a time before settling.

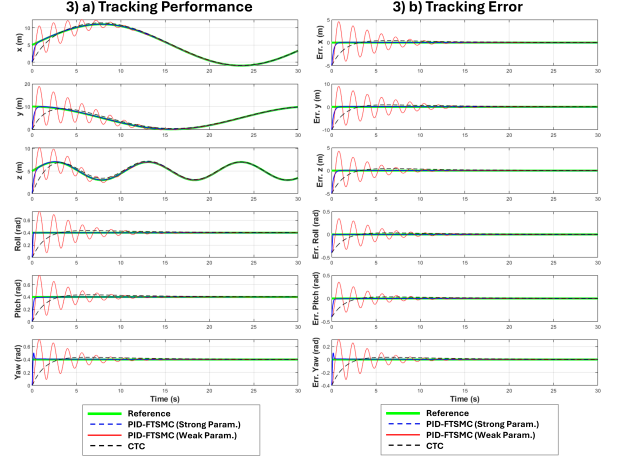


Fig. 3. PID-FTSMC 6DOF Tracking Performance and Error (PID-FTSMC vs. CTC)

Figure 4 provides insights into the velocities and control signals for each 6DOF throughout the simulation. Initially stationary, the AUV's velocity spikes to 20 m/s and 3 rad/s quickly. Since the BlueRov2 cannot achieve such high velocities, the motion to the reference concludes rapidly. This unrealistic behaviour can be managed by limiting the control signals, which will be explored in future work. The plots show no oscillation in control signals once the reference is met. For comparison, both the CTC's and badly-tuned PID-FTSMC's control signals and velocities are plotted.

5. CONCLUSIONS

In this paper, a novel PID-FTSMC controller has been developed and simulated for the trajectory tracking of AUVs under the influence of disturbances. The proposed controller merges the advantages of PID control with FTSMC to address common challenges such as chattering, slow convergence, and robustness against uncertainties.

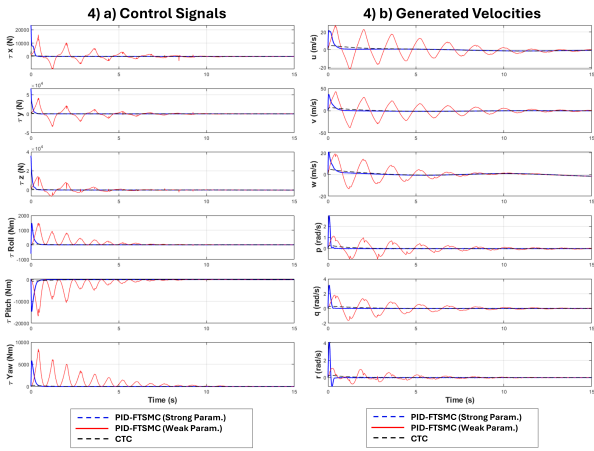


Fig. 4. PID-FTSMC 6DOF Velocities and Control Signals (PID-FTSMC vs. CTC)

The simulation results, performed on a 6DOF BlueRov2, confirm the effectiveness of the PID-FTSMC controller. The controller - given suitable gains - ensured fast, smooth convergence to the desired trajectory without chattering, even in the presence of external disturbance. The stability of the proposed controller was rigorously analysed and proven, showcasing its ability to maintain tracking and eliminate the chattering phenomenon. Despite the positive results, some areas for improvement were highlighted, such as the optimal tuning of controller parameters and the constraint of control signals to achieve realistic velocities. Future work will focus on addressing these limitations through implementing Reinforcement Learning.

REFERENCES

- Ajmal, M.S., Labeeb, M., and Dev, D.V. (2014). Fractional order pid controller for depth control of autonomous underwater vehicle using frequency response shaping approach. In *IEEE*. doi:10.1109/aicera.2014.6908219. URL <https://dx.doi.org/10.1109/aicera.2014.6908219>.
- Bellingham, J.G. (2009). Platforms: Autonomous underwater vehicles. doi:10.1016/B978-012374473-9.00730-X. URL <https://doi.org/10.1016/B978-012374473-9.00730-X>.
- Bharti, V., Lane, D., and Wang, S. (2018). Robust subsea pipeline tracking with noisy multibeam echosounder. In *IEEE*. doi:10.1109/auv.2018.8729803. URL <https://dx.doi.org/10.1109/auv.2018.8729803>.
- Boiko, I. (2023). *Chattering in Mechanical Systems Under Sliding-Mode Control*. Springer International Publishing.
- Fossen, T.I. (2011). *Handbook of Marine Craft Hydrodynamics and Motion Control*. Wiley. doi:10.1002/9781119994138.
- Gomez, D., Lopez, A., Tombe, J., and Romero Cano, V. (2020). Design of a sliding mode control for an autonomous underwater vehicle. In *IEEE*. doi:10.1109/ciima50553.2020.9290182. URL <https://dx.doi.org/10.1109/ciima50553.2020.9290182>.
- Horimoto, H., Maki, T., Kofuji, K., and Ishihara, T. (2018). Autonomous sea turtle detection using multi-beam imaging sonar: Toward autonomous tracking. In *IEEE*. doi:10.1109/auv.2018.8729723. URL <https://dx.doi.org/10.1109/auv.2018.8729723>.
- Knight, R. (2024). Militaries are taking unmanned underwater. URL <https://insideunmannedsystems.com/militaries-are-taking-unmanned-underwater/>.
- Lipko, I. (2023). Pid based path following algorithm for the middleauv. In *IEEE*. doi:10.1109/icieam57311.2023.10138983. URL <https://dx.doi.org/10.1109/icieam57311.2023.10138983>.
- Liu, L., Zhang, L.C., Pan, G., and Zhang, S. (2022). Robust yaw control of autonomous underwater vehicle based on fractional-order pid controller. *Ocean Engineering*, 257. doi:10.1016/j.oceaneng.2022.111493.
- Mudassir, M. and Memon, A.Y. (2020). Steering control of an autonomous underwater vehicle using smc techniques. In *IEEE*. doi:10.1109/iccr51572.2020.9344394. URL <https://dx.doi.org/10.1109/iccr51572.2020.9344394>.
- Qin, H.D., Si, J.S., Wang, N., and Gao, L.Y. (2023). Fast fixed-time nonsingular terminal sliding-mode formation control for autonomous underwater vehicles based on a disturbance observer. *Ocean Engineering*, 270. doi:10.1016/j.oceaneng.2022.113423.
- Sarhadi, P., Noei, A.R., and Khosravi, A. (2016). Model reference adaptive pid control with anti-windup compensator for an autonomous underwater vehicle. *Robotics and Autonomous Systems*, 83, 87–93. doi:10.1016/j.robot.2016.05.016.
- SNAME (1950). Nomenclature for treating the motion of a submerged body through a fluid. Report.
- Tang, J., Dang, Z.K., Deng, Z.C., and Li, C.Q. (2022). Adaptive fuzzy nonlinear integral sliding mode control for unmanned underwater vehicles based on eso. *Ocean Engineering*, 266. doi:10.1016/j.oceaneng.2022.113154.
- Van, M. (2019a). Adaptive neural integral sliding-mode control for tracking control of fully actuated uncertain surface vessels. *International Journal of Robust and Nonlinear Control*, 29(5), 1537–1557. doi:10.1002/rnc.4455.
- Van, M. (2019b). An enhanced tracking control of marine surface vessels based on adaptive integral sliding mode control and disturbance observer. *ISA Transactions*, 90, 30–40. doi:10.1016/j.isatra.2018.12.047.
- Van, M., Kang, H.J., and Shin, K.H. (2014). Novel quasi-continuous super-twisting high-order sliding mode controllers for output feedback tracking control of robot manipulators. *Proceedings of the Institution of Mechanical Engineers, Part C: Journal of Mechanical Engineering Science*, 228(17), 3240–3257. doi:10.1177/0954406214526828.
- Van, M., Sun, Y., McIlvanna, S., Nguyen, M.N., Khyam, M.O., and Ceglarek, D. (2023). Adaptive fuzzy fault tolerant control for robot manipulators with fixed-time convergence. *IEEE Transactions on Fuzzy Systems*, 31(9), 3210–3219. doi:10.1109/tfuzz.2023.3247693.
- Zhu, Z., Wu, Z., Deng, Z., Qin, H., and Wang, X. (2018). An ocean bottom flying node auv for seismic observations. In *IEEE*. doi:10.1109/auv.2018.8729726. URL <https://dx.doi.org/10.1109/auv.2018.8729726>.
- Zhu, Z.B., Duan, Z.Q., Qin, H.D., and Xue, Y.F. (2023). Adaptive neural network fixed-time sliding mode control for trajectory tracking of underwater vehicle. *Ocean Engineering*, 287. doi:10.1016/j.oceaneng.2023.115864.